Qeios

Dynamic structure factors and equation of state of fluid iron under Earth's core condition

Wei-Jie Li[1], Zi Li[2,5], Jie Zhou[1], Hao Ma[3], Yi-Xiao Li[4], Qian Jia[4], Zhe Ma[1], Cong Wang[2,5,6], Ping Zhang[2,5,6]

[1] Intelligent Science & Technology Academy Limited of CASIC, Beijing, 100141, People's Republic of China
[2] Institute of Applied Physics and Computational Mathematics, Beijing, 100088, People's Republic of China
[3] School of Mechanical and Electric Engineering, Sanming University, Sanming, 365004, China
[4] The Second Academy of CASIC, Beijing, 100854, People's Republic of China
[5] Tianfu Innovation Energy Establishment, Chengdu, 610213, China
[6] Center for Applied Physics and Technology, Peking University, Beijing, 100871, People's Republic of China

Abstract

The geodynamo is crucial for the activity of Earth's outer core, which is mainly made of fluid iron. The *ab initio* molecular dynamics were adopted on the calculations of ion-ion dynamic structure factors and the equations of states of pure iron under Earth's core condition. The calculated static structure factors, ion-ion dynamic structure factors, and dispersion curve of pure iron were consistent with the reported *in situ* x-ray diffraction and inelastic x-ray scattering measurements. A multivariate polynomial method based on the ab initio calculated pressure-volume-temperature data was proposed in the formulation of the equations of states with high accuracy, by which the pressure and temperature dependent thermoelastic properties can be directly calculated by definitions. From the isentropic profiles in the Earth's outer core, the iron exhibited about 10% higher density, 7% lower sound velocity, and an almost identical adiabatic bulk modulus when compared to the preliminary reference Earth model. The adiabatic sound velocities calculated by dynamic structure factors and the equations of states methods were physically equivalent. However, the sound velocity of iron calculated by the fitted equation of state is about 5% lower than that by the dynamic structure factors method.

Keywords: structure factors; equation of state; sound velocity; Earth's core; ab initio calculation

1. Introduction

The equations of states (EOS), longitudinal sound velocity (V_P), and density are of great importance to in understanding Earth's and terrestrial planets' core composition behavior. The V_P is a crucial physical quantity and directly correlated with the seismic wave. The dynamic structure factor is also crucial for the x-ray experiment to get an insight into the properties of matter and was recently reported to get the EOS of liquid Fe liquid experimentally (Kuwayama et al., 2020). Here, we calculate the dynamic structure factors and EOS by ab initio molecular dynamic simulations separately and compared the numerical accuracy of V_P derived from both the calculated dynamic structures factors and EOS methods.

The calculation of V_P is usually derived from the EOS or elastic constants. The elasticity and V_P of Earth's interiors were first established by Birch (Birch, 1952), and the definitions of the thermoelastic properties were supplied. Then, the Birch-Murnaghan finite strain EOS of Fe were presented based on the ultrasonic, thermal expansion, and enthalpy data at 1 bar and on pulse-heating and shock wave

https://doi.org/10.32388/YZ6RIT

compression and sound speed data up to 10 Mbar (Anderson and Ahrens, 1994). The EOS and thermoelastic properties were calculated by ab initio molecular dynamic simulations and Vinet (Morse-Rydberg) equation combined with the quasi-harmonic Debye model (Ichikawa et al., 2014). It showed that the density and adiabatic bulk modulus of pure liquid iron was found to be 8-10% and 3-10% larger than the preliminary reference Earth model (PREM) values (Dziewonski and Anderson, 1981), and the V_P agreed well (Ichikawa et al., 2014). The V_P and bulk modulus of liquid iron binaries were calculated by ab initio simulations combined with the Birch-Murnaghan EOS (Badro et al., 2014; Brodholt and Badro, 2017), which showed that Ni addition decreased V_P while other light elements addition increased V_P. The ab initio molecular dynamic simulations were also conducted on the iron-hydrogen alloys, and showed that both the density and V_P of liquid iron containing ~1 wt.% hydrogen match seismological observations (Umemoto and Hirose, 2015). On the other hand, the elastic constants tensor were calculated by the first-principle simulations to observe hydrogen effect on solid iron, and showed that hydrogen was an undesirable light element in the Earth's core to match the seismological observations (Caracas, 2015).

The experimental methods of the V_P include derive from the phonon density of state (Mao et al., 2001) and structure factors (Kuwayama et al., 2020). The nuclear resonant inelastic x-ray scattering measured Fe to 153 GPa, and then the Debye average phonon velocity was obtained by the phonon density of state (Mao et al., 2001). The thermoelastic properties were determined by nuclear resonant inelastic x-ray scattering and calculated from ab initio theory, which agreed well with each other (Mao et al., 2001). The V_P was obtained to 45 GPa and 2700 K based on inelastic x-ray scattering measurement (Kuwayama et al., 2020), then the Mie-Grüneisen EOS for liquid Fe was determined by results and previous shock-wave data. It indicated that Earth's outer core exhibited 7.5%-7.6% density deficit, 3.7%-4.4% velocity excess, and an almost identical adiabatic bulk modulus (Kuwayama et al., 2020). The EOS and V_P of Fe-S fluid under Martian core conditions were measured using the ultrasonic pulse-echo overlap method combined with a Kawai-type multi-anvil apparatus up to 20 GPa (Nishida et al., 2020). The EOS was expressed by the adiabatic third-order Birch-Murnaghan EOS, and the V_P was derived by its definition (Nishida et al., 2020). The traditional EOS was derived from empirical equations, such as Birch-Murnaghan EOS (Anderson and Ahrens, 1994; Birch, 1952) and Mie-Grüneisen EOS (Kuwayama et al., 2020).

The structure factors have also been calculated by orbital-free density-function theory simulation (White et al., 2013), molecular dynamics (Liu et al., 2020), and ab initio molecular simulations (Gill et al., 2015; Rüter and Redmer, 2014; Witte et al., 2017). The ab initio calculation of ion-ion dynamic structure factors includes warm dense Al (Rüter and Redmer, 2014), warm dense lithium (Witte et al., 2017), and mixture (Gill et al., 2015). Then, the V_P is the slope of the dispersion relation for small wave vectors, which is determined by analyzing the position of the side peaks of dynamic structure factors. The V_Ps of Fe-Ni-O liquid were calculated by ion-ion dynamic structure factors and ab initio molecular dynamics simulations, and the results showed that V_P of the Fe-Ni-O liquid was lower at the core-mantle boundary (CMB) and high at the inner-core boundary (ICB) than PREM values (Li et al., 2023). The calculated structure factors can be compared with available experimental x-ray and neutron scattering data. However, the *ab initio* calculated structure factors under Earth's core condition have never been compared with experimental results, and the calculation accuracy of V_P is

not verified.

The methods of the V_P include EOS or elastic constants from independent DFT calculation and dynamic structure factors. In this paper, the *ab initio* molecular dynamics simulations were adopted in the calculation of the dynamic structures and EOS of liquid Fe. The static structure factors and radial distribution function were compared with the experimental data. The dynamic structure factors and dispersion curve were calculated, and then the V_Ps at the specified states were collected. The EOS of pure Fe was fitted by multivariate polynomial method via separate ab initio molecular dynamics runs, and then the thermoelastic properties and isentropic profiles of Earth's outer core were collected by definitions. At last, the thermoelastic properties under Earth's conditions were compared with PREM values, and the calculated V_Ps by the two methods were analyzed.

2. Methods and Calculations

2.1. Structure factors

A detailed illustration of structure factors is shown in (Hansen and McDonald, 2006). The dynamic structure factors are the spectral function of the density-density correlations in the system. The ion density in Fourier space

$$\rho_{\mathbf{q}}^{i}(t)=\sum_{v=1}^{N} e^{-i\mathbf{q}\mathbf{r}_v(t)}, \tag{1}$$

where $\mathbf{q}$ is the wave number, N is the total number of particles, and $\mathbf{r}_v(t)$ is the vth ion position at time t.

The intermediate scattering function $F_{ii}(\mathbf{q},t)$ is defined as

$$F_{ii}(\mathbf{q},t) \coloneqq \frac{1}{N}\lim_{T\to\infty}\frac{1}{T}\int_0^T \rho_{\mathbf{q}}^{i}(\tau)\rho_{-\mathbf{q}}^{i}(t+\tau)d\tau. \tag{2}$$

The dynamic structure factor is calculated via the intermediate scattering function $F_{ii}(\mathbf{q},t)$. The ion-ion dynamic structure factor $S_{ii}(\mathbf{q},\omega)$ is defined as the Fourier transform of the intermediate scattering function

$$S_{ii}(\mathbf{q},\omega) \coloneqq \frac{1}{2\pi}\int_{-\infty}^{\infty} F_{ii}(\mathbf{q},t)e^{i\omega t}dt, \tag{3}$$

where the ω denotes the frequency. The ion-ion dynamic structure factor S(q,ω) characterizes the collective dynamics of fluctuations of ionic density over both length and time scales. The S(q,ω) can be measured by inelastic x-ray scattering experiments (Kuwayama et al., 2020). By collecting the peak positions of S(q,ω) at different wave vectors q, the dispersion relation is obtained. The V_P is the slope of the dispersion relation at small wave vectors, $d\omega/dq|_{q\to 0}$. On the other hand, the sound velocity can be calculated directly by the EOS (shown in Section 2.2). Theoretically, the sound velocities calculated by EOS and dynamic structure factors are equal.

The static structure factor is obtained via the intermediate scattering function

$S_{ii}(\mathbf{q}) = F_{ii}(\mathbf{q}, 0)$. The isothermal bulk modulus (K_T) can be computed from S(q) at $q \rightarrow 0$ with the form (Hansen and McDonald, 2006) of

$$S_{ii}(q \rightarrow 0) = \frac{n_i k_B T}{K_T}, \tag{4}$$

where $n_i = N/V$ is the ionic density, k_B is the Boltzmann constant and T is the temperature. The isothermal bulk modulus can also be determined from the EOS via separate ab initio molecular dynamics runs.

To be pointed out, *S(q)* is the Fourier transformation of radial distribution function *g(r)*. The radial distribution function *g(r)* is defined as

$$g(r) = \frac{V}{4\pi r^2 N^2} \left\langle \sum_{i=1}^{N} \sum_{j=1, j \neq i}^{N} \delta\left(r - \left|\mathbf{r}_i - \mathbf{r}_j\right|\right) \right\rangle, \tag{5}$$

where V is the cell volume, N is the number of atoms, r_i, and r_j are atomic coordinates of atoms i and j, and <…> means the time or ensemble average.

2.2. Equations of states

Traditionally, the EOS of Fe or its alloy under Earth's core condition is described by empirical equations (such as Birch-Murnaghan EOS and Mie-Gruneisen EOS), and then its thermoelastic properties were collected. In this paper, we adopted a fitting method on EOS based on pressure-volume-temperature (P-V-T data) and energy-volume-temperature (E-V-T) data, then the thermo-elastic properties were calculated by definitions directly.

Based on the hundreds of P-V-T data and E-V-T data, the EOS is

$$\begin{aligned} P &= \sum_{i,j} A_{ij} V^i T^j, \\ E &= \sum_{i,j} B_{ij} V^i T^j, \end{aligned} \tag{6}$$

where A_{ij} and B_{ij} are the fitted parameters of pressure and energy, respectively.
The definition of thermal expansion coefficient α is

$$\alpha = \frac{1}{V}\left(\frac{\partial V}{\partial T}\right)_P. \tag{7}$$

The specific heat capacity at constant volume C_V is

$$C_V = \left(\frac{\partial E}{\partial T}\right)_V. \tag{8}$$

The isothermal bulk modulus K_T is

$$K_T = -V\left(\frac{\partial P}{\partial V}\right)_T. \tag{9}$$

The thermodynamic Gruneisen parameter γ is defined by

$$\gamma = V\left(\frac{\partial P}{\partial E}\right)_V . \tag{10}$$

The adiabatic bulk modulus K_S is

$$K_S = \left(1+\alpha\gamma T\right)K_T, \tag{11}$$

where α is the coefficient of thermal expansion, and γ is the Grüneisen parameter. To be pointed out, K_T and K_S depend on both temperature and pressure.

The adiabatic sound velocity V_P of liquid is

$$V_P\left(P,T\right) = \sqrt{\frac{K_S\left(P,T\right)}{\rho\left(P,T\right)}}. \tag{12}$$

The isentropic temperature profile T_{ad} is given by the following thermodynamic relationships as

$$\left(\frac{\partial T_{ad}}{\partial P}\right)_S = \frac{\alpha V T_{ad}}{C_P} = \frac{\gamma T_{ad}}{K_S}, \tag{13}$$

where C_P is isobaric heat capacity. An isentropic temperature profile referred to as geotherm is obtained by integrating Eq. (13) with the Gruneisen parameter γ for liquid Fe. The pressure at ICB is 329 GPa, and the temperatures at the ICB are selected as 5000 K, 5500 K, and 6000 K. Then, the thermoelastic properties along the geotherm are collected by the isentropic pressure and temperature profiles.

2.3. Calculation details

The *ab initio* molecular dynamics calculations are implemented in the plane wave density functional VASP code (Kresse and Furthmüller, 1996; Kresse and Hafner, 1993). In this calculation, projector augmented waves (PAWs) (Blöchl, 1994; Kresse and Joubert, 1999) and generalized gradient approximation (GGA) in the parameterization of Perdew, Burke, and Ernzerhof (Perdew et al., 1996) are adopted. The pseudopotential of Fe has p electrons as valence electrons. The plane wave cutoff is 500 eV, which is sufficient to ensure that the pressure converges within 1% accuracy. The time-dependent mean square displacement is employed to check the system in the liquid state. The selected time step is 1 fs. In the calculation of structure factors, we selected 128 atoms as the cell, and Fe atoms were randomly distributed in the cell. First, the NPT ensemble is calculated for 2000 time steps, and then the equilibrium volume is computed under certain pressures and temperatures. Then, the long-term correlation function is collected by the *NVT* ensemble with the equilibrium volume. When the total time exceeds 20 ps, the convergence ion-ion structure factors are obtained. In the calculation of EOS, we selected 64 atoms as the cell. The MD simulation with NVT ensemble was executed for a total of 6 ps with the last 3 ps considered as the production run, where the total energy and pressure fluctuations were less than 1%.

3. Results and discussions

3.1. Structure factors

The static structure factors *S(q)* and radial distribution function *g(r)* of Fe under the

Earth's core condition were collected in Figure 1. The shapes of *S(q)* and *g(r)* were similar to the reported experimental data, which was obtained from the *in situ* x-ray diffraction measurements (Kuwayama et al., 2020). From the calculations of *S(q)* and *g(r)*, it was obvious that was liquid. When the temperature was lower, the liquid Fe may be solidification, and the shapes of *S(q)* and *g(r)* should be changed. Note that the smallest q available in *S(q)* is determined by $2\pi/a$ with a being the lattice constant of the simulation supercell, and the structure factor at small q represents the long-ranged structural information of systems. The K_T can be calculated from *S(q)* at $q \rightarrow 0$ with the form of Eq. (4). In order to accurately compute K_T, larger supercells were needed to obtain *S(q)* at small q. As the limited size of the supercells in the ab initio molecular dynamics simulations, the K_T was not calculated by *S(q)* and just calculated by EOS in Section 3.2.

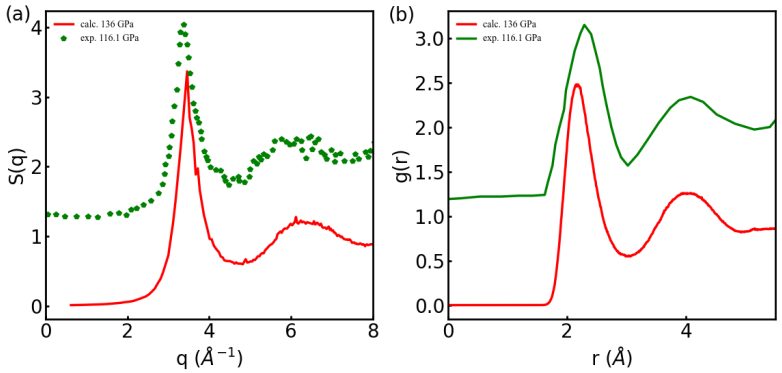

Figure 1 The static structure factor *S(q)*, and radial distribution function *g(r)* of liquid Fe. The 'calc. 136 GPa' label was ab initio simulations data. The 'exp. 116.1 GPa' label was structural analyses of liquid Fe via *in situ* x-ray diffraction measurements (Kuwayama et al., 2020), and was shifted up.

The ion-ion dynamic structure factors were calculated by Eq.(3). The ion-ion dynamic structure factors *S(q,ω)* at different wave vectors **q**s at 136 GPa and 330 GPa were shown in Figure 2. The shape of the calculated ion-ion dynamic structure factors was similar to the reported high-pressure inelastic x-ray scattering measurements of liquid Fe (Kuwayama et al., 2020). There is a central Rayleigh peak and two ion acoustic modes are observed in *S(q,ω)*. The ion acoustic modes are the Stoke and anti-Stoke peak. The sound velocities were derived by the dispersion relations of the ion acoustic modes. Figure 2 mainly provided the ion acoustic modes information of *S(q,ω)*. As the **q**s increased, the peaks of *S(q,ω)* moved to the high ω and then move back to the low ω.

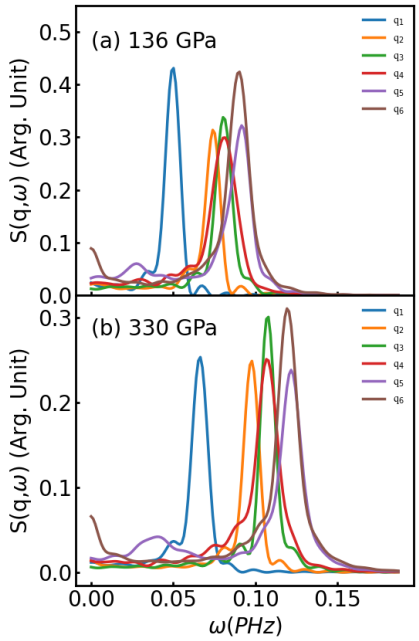

Figure 2 The ion-ion dynamic structure factors *S(q,ω)* of Fe liquid under Earth's core conditions. (a) is at 136 GPa and 4000 K, and (b) is at 330 GPa and 5500 K. The 'q_i' labels are wave numbers with $q_i=2\pi\sqrt{i}/a$ (i=1,2…), where a is the equilibrium lattice parameters at the specified state.

The adiabatic sound velocities along the geotherm curve can also be collected by long-time ab initio molecular dynamics simulations. By collecting the peak positions of S(q,ω) at different wave vectors, the dispersion curves of Fe liquid at specified temperature and pressure states were obtained and plotted in Figure 3. The adiabatic sound velocity V_P is the slope of the linear part of the dispersion curve at long wavelengths. The adiabatic sound velocity of Fe liquid at CMB was 8.38 km/s and at ICB was 10.46 km/s. As q increases, the correlation scale is reduced below that of the repulsion, the dispersion curves diverge. The accuracy of the V_P is closely correlated with the energy cutoff, number of ions, time step and number of time steps.

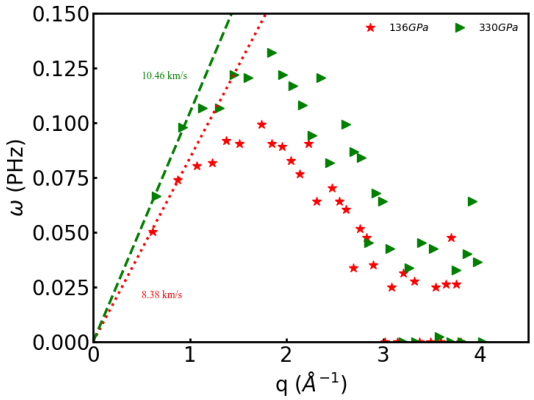

Figure 3 Dispersion curve and adiabatic sound velocity of Fe liquid under the Earth's core condition. The dispersion curves were directly derived from Figure 2.

3.2. Equation of state

From the ab initio molecular dynamics simulations, the pressure and energy at specified volume and temperature states (NVT ensemble) were collected. By using the sklearn package in python programming language, the EOS was fitted by Eq. (6) within 0.5% accuracy. The fitting parameters of EOS by fitting Eq.(6) were shown in Table 1. From the fitted EOS, the isothermal bulk modulus K_T and adiabatic sound velocity V_P at specified temperature and pressure state were calculated by Eqs.(9) and (12), shown in Figure 4. The numerical results of K_T and V_P were consistent with the reported seismic (Dziewonski and Anderson, 1981; Garnero et al., 1993) and calculated data (Anderson and Ahrens, 1994; Birch, 1952; Kuwayama et al., 2020). The thermoelastic properties were usually derived by the empirical Birch-Murnaghan EOS (Anderson and Ahrens, 1994; Birch, 1952) and Mie-Gruneisen EOS (Kuwayama et al., 2020). Our calculated data about K_T and V_P verified the feasibility and effectiveness of our proposed multivariate polynomial method about the EOS.

Table 1 The fitting parameters of pressure and energy of pure Fe liquid under Earth's core condition calculated by Eq.(6).

A_{ij}	$i=0$	$i=1$	$i=2$	B_{ij}	$i=0$	$i=1$	$i=2$
$j=0$	444.84	-0.011	1.54	j=0	-0.806	-1.59×10^{-4}	5.83×10^{-8}
$j=1$	-115.12	0.00083	0	j=1	-1.416	2.26×10^{-6}	0
$j=2$	7.76	0	0	j=2	0.0826	0	0

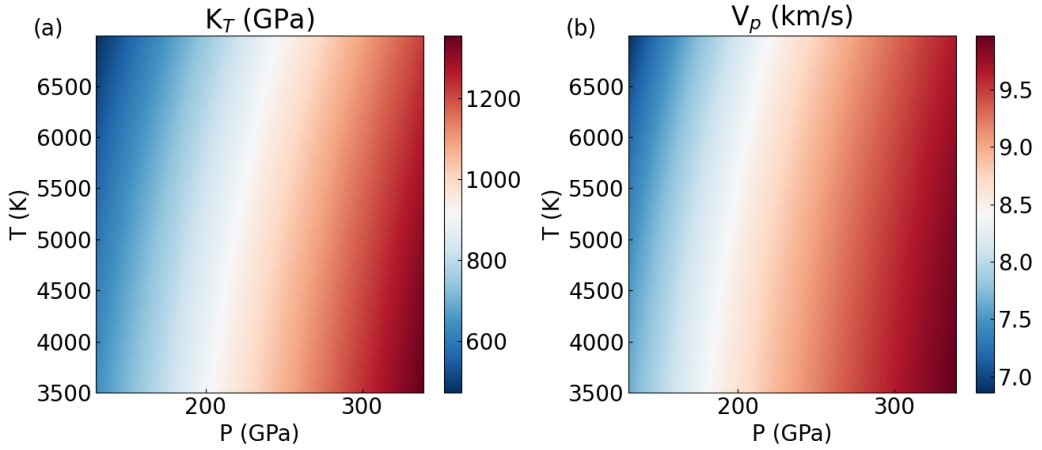

Figure 4 The ab initio calculated (a) isothermal bulk modulus K_T and (b) adiabatic sound velocity V_P at different temperature and pressure states.

3.3. Properties of Earth's core

The geotherm curve was calculated by Eq. (13) and the fitted EOS. The isentropic temperature T_{ad} and density ρ profile were calculated with three different ICB conditions (T_{ICB}=5000 K, 5500 K, 6000 K), shown in Figure 5 (a) and (b). For the same ICB temperature (5000 K), the T_{ad} at CMB calculated by the fitted EOS was 6.46% lower than the Mie-Grüneisen EOS by experimental data (Kuwayama et al., 2020)

and 5.88% lower than EOS (Anderson and Ahrens, 1994). The density ranged from 11.04 g/cm^3 to 13.25 g/cm^3 when T_{ICB}=5500 K. The density was about 10% higher than the PREM density value (Dziewonski and Anderson, 1981), which implied the existence of light elements. The density difference between our fitted data and the Mie-Grüneisen EOS by experimental data (Kuwayama et al., 2020) was within 3%. The adiabatic sound velocities calculated by EOS were both lower than the PREM values and calculated by the dispersion curve.

After the geotherm curve was confirmed, the isentropic bulk modulus K_S and (d) adiabatic sound velocity V_P were collected in Figure 5 (c) and (d). The K_S ranged from 657.05 GPa to 1259.92 GPa when T_{ICB} = 5500 K, which was consistent with the PREM values (Dziewonski and Anderson, 1981). The temperature and pressure profiles in the calculation of ion-ion dynamic structure factors in Section 3.1 were also the geotherm curve with T_{ICB} = 5500 K. The V_P along the geotherm ranged from 7.71km/s to 9.75 km/s by the EOS method and ranged from 8.38 km/s to 10.46 km/s by dynamic structure factors. The reported V_P of Al calculated by dynamic structure factors agreed with experimental data within 6% (Rüter and Redmer, 2014). The sound velocity calculated by fitted EOS were coincided with the Mie-Grüneisen EOS by experimental data (Kuwayama et al., 2020).

Though the V_P calculated by the EOS and dynamic structure factors are physically equivalent, the difference between the calculated V_Ps by these two methods was about 5%. When the V_Ps compared with the PREM values, the two methods may give different conclusions. The size of the supercell in the dynamic structure factors calculations was only 128 atoms, which would affect the accuracy of V_P. The lattice parameter decided the number of **q** in the dispersion curves, which would directly affect the fitting accuracy of V_P at small **q**s. The equivalent of the sound velocity calculated by dynamic structure factors and EOS are verified, but not applicable to small accurate difference analysis. When a sound velocity at a specified state is needed, ab initio molecular dynamic simulations about the dynamic structure factors with a large supercell is appropriate, which calculated a long-time simulation with only one calculation. When sound velocity in a wide temperature and pressure range are needed, the ab initio molecular dynamic simulations about the EOS with a relatively small supercell (64 atoms for example) were appropriate, which calculated relatively short-time simulations with hundreds of calculations.

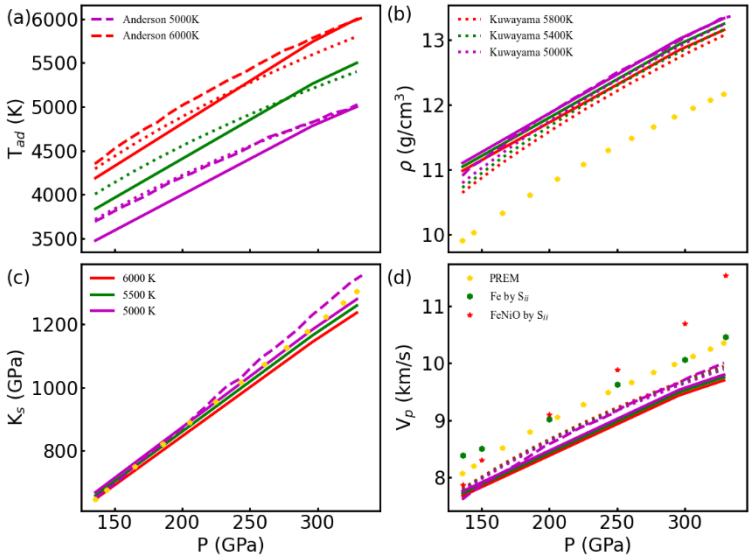

Figure 5 The geotherm profiles of liquid Fe under Earth core condition. (a) isentropic temperature T_{ad}, (b) density ρ, (c) adiabatic bulk modulus K_S and (d) adiabatic sound velocity V_P. The ICB temperatures were selected as 5000 K, 5500 K, and 6000 K, respectively. 'Experimental data' (Kuwayama et al., 2020), 'PREM values' were data from PREM (Dziewonski and Anderson, 1981). 'FeNiO by Sii' was from (Li et al., 2023), and the label 'Anderson XXX' was from (Anderson and Ahrens, 1994). The four subfigures shared the lables.

4. Conclusions

The static structure factors, ion-ion dynamic structure factors, and EOS of Fe under the Earth's core condition were calculated by the ab initio molecular dynamics simulations. Then, the sound velocities of Fe are calculated by both dynamic structure factors and EOS, which are physically equivalent. The V_P of pure Fe under Earth's core condition ranged from 7.71km/s to 9.75 km/s by the EOS method and ranged from 8.38 km/s to 10.46 km/s by dynamic structure factors method. Ab initio molecular dynamics simulations make a supplement for the higher energy x-ray to collect diffuse signals in a wider **q** range. The calculation of structure factors opened a way that can be compared to the high pressure *in situ* x-ray diffraction and inelastic x-ray scattering measurements.

Acknowledgement

This work was support by the National Natural Science Foundation of China (NSFC) [grant numbers 11975058, 11775031 and 11625415], and the fund of Key Laboratory of Computational Physics [grant number 6142A05RW202103]. We thanked for the fund support from Laboratory of Computational Physics in Institute of Applied Physics and Computational Mathematics.

Data availability

The data from this paper are available on reasonable request to Wei-Jie Li (liweijie8680@126.com).

References

Anderson, W.W., Ahrens, T.J., 1994. An equation of state for liquid iron and implications for the Earth's core. Journal of Geophysical Research: Solid Earth 99, 4273-4284.

Badro, J., Côté, A.S., Brodholt, J.P., 2014. A seismologically consistent compositional model of Earth's core. Proceedings of the National Academy of Sciences 111, 7542-7545.

Birch, F., 1952. Elasticity and constitution of the Earth's interior. Journal of Geophysical Research 57, 227-286.

Blöchl, P.E., 1994. Projector augmented-wave method. Physical Review B 50, 17953.

Brodholt, J., Badro, J., 2017. Composition of the low seismic velocity E layer at the top of Earth's core. Geophysical Research Letters 44, 8303-8310.

Caracas, R., 2015. The influence of hydrogen on the seismic properties of solid iron. Geophysical Research Letters 42, 3780-3785.

Dziewonski, A.M., Anderson, D.L., 1981. Preliminary reference Earth model. Physics of the earth planetary interiors 25, 297-356.

Garnero, E.J., Helmberger, D.V., Grand, S.P., 1993. Constraining outermost core velocity with SmKS waves. Geophysical Research letters 20, 2463-2466.

Gill, N.M., Heinonen, R.A., Starrett, C.E., Saumon, D., 2015. Ion-ion dynamic structure factor of warm dense mixtures. Physical Review E 91, 063109.

Hansen, J.-P., McDonald, I.R., 2006. Theory of simple liquids. Elsevier.

Ichikawa, H., Tsuchiya, T., Tange, Y., 2014. The P-V-T equation of state and thermodynamic properties of liquid iron. Journal of Geophysical Research: Solid Earth 119, 240-252.

Kresse, G., Furthmüller, J., 1996. Efficient iterative schemes for ab initio total-energy calculations using a plane-wave basis set. Physical Review B 54, 11169.

Kresse, G., Hafner, J., 1993. Ab initio molecular dynamics for liquid metals. Physical Review B 47, 558.

Kresse, G., Joubert, D., 1999. From ultrasoft pseudopotentials to the projector augmented-wave method. Physical Review B 59, 1758.

Kuwayama, Y., Morard, G., Nakajima, Y., Hirose, K., Baron, A.Q.R., Kawaguchi, S.I., Tsuchiya, T., Ishikawa, D., Hirao, N., Ohishi, Y., 2020. Equation of State of Liquid Iron under Extreme Conditions. Physical Review Letters 124, 165701.

Li, W.-J., Li, Z., Mo, C.-J., Ma, Z., He, X.-T., Wang, C., Zhang, P., 2023. Self-diffusion coefficient and sound velocity of Fe-Ni-O fluid: Implications for the stratification of Earth's outer core. Physics of the Earth and Planetary Interiors, 106983.

Liu, Q., Lu, D., Chen, M., 2020. Structure and dynamics of warm dense aluminum: a molecular dynamics study with density functional theory and deep potential. Journal of Physics: Condensed Matter 32, 144002.

Mao, H., Xu, J., Struzhkin, V., Shu, J., Hemley, R., Sturhahn, W., Hu, M., Alp, E., Vocadlo, L., Alfè, D., 2001. Phonon density of states of iron up to 153 gigapascals. Science 292, 914-916.

Nishida, K., Shibazaki, Y., Terasaki, H., Higo, Y., Suzuki, A., Funamori, N., Hirose, K., 2020. Effect of sulfur on sound velocity of liquid iron under Martian core conditions. Nature Communications 11, 1954.

Perdew, J.P., Burke, K., Ernzerhof, M., 1996. Generalized gradient approximation made simple. Physical Review Letters 77, 3865.

Rüter, H.R., Redmer, R., 2014. Ab initio simulations for the ion-ion structure factor of warm dense aluminum. Physical Review Letters 112, 145007.

Umemoto, K., Hirose, K., 2015. Liquid iron-hydrogen alloys at outer core conditions by first-principles calculations. Geophysical Research Letters 42, 7513-7520.

White, T., Richardson, S., Crowley, B., Pattison, L., Harris, J., Gregori, G., 2013. Orbital-free density-functional theory simulations of the dynamic structure factor of warm dense aluminum. Physical Review Letters 111, 175002.

Witte, B., Shihab, M., Glenzer, S., Redmer, R., 2017. Ab initio simulations of the dynamic ion structure factor of warm dense lithium. Physical Review B 95, 144105.